ZANCO Journal of Pure and Applied Sciences

TYPE Original article
DOI http://dx.doi.org/10.21271/ZJPAS.37.5.6

OPEN ACCESS

*Corresponding author

Kaifi Chomani
Kaifi.chomani@gmail.com

RECEIVED :14 /12 /2024
ACCEPTED :20/04/ 2025
PUBLISHED :31/ 10/ 2025

KEYWORDS:

Flood vulnerability, GIS, Analytical Hierarchy Process, flood risk zones, urban planning, Erbil city.

Urban Building Flood Vulnerability Assessment in Erbil City: A Geospatial and AHP-Based Approach

Kaifi Chomani[1, 2*], Dleen Mohammed Saleh Al-shrafany[1]

1Department of Geomatics (Surveying) Engineering, College of Engineering, Erbil, Salahaddin University-Erbil, Erbil ,Kurdistan Region, Iraq
2Civil Engineering Department, University of Raparin, Ranya, Sulaymaniyah, Iraq.

ABSTRACT

The frequency and intensity of flash floods increased substantially in recent years in the world which are the major risk for urban regions and environment. The objective of this comprehensive study is to assess the buildings vulnerable to flood hazards in Erbil city, Kurdistan region of Iraq using the integrated approaches of Geographic Information Systems (GIS), satellite remote sensing, and the Analytical Hierarchy Process (AHP). 14 flood-contributing parameters were used to map flood susceptible regions in the Erbil city. Rainfall, aspect, topographic wetness index (TWI), elevation, flow accumulation, lithology, soil data, normalized difference vegetation index (NDVI), normalized difference built-up index (NDBI), land use land cover (LULC), slope, stream power index (SPI), drainage density, and distance to roads were the factors that have been used to create flood susceptibility map (FSM). The FSM map showed considerable results with the accuracy of the 92.2%, using historical flood data to assess the accuracy. The results showed that 109 km2 (12.1%) of Erbil city area located in high and very high flood risk areas. Moreover, the outcome underscored startling results, showing that nearly half of buildings in Erbil city (47.6%) were located in high or very high flood risk areas. Additionally, the finding showed that 33853 (3.84%) and 69258 (7.85%) of population in Erbil city were located in very high and high risk flood zones, respectively. This study offers valuable insights for policy makers and urban planners, significantly contributing in monitoring urban environments, early warning systems, flood mitigation strategies and sustainable urban growth.

1. Introduction

The technological innovations in flood hazard assessment significantly contributed in better understanding the primary factors and mitigating the impact of flood hazards, specifically in urban areas. Floods can have severe impact such as infrastructure damages, risking public safety and daily life disturbance (Samansiri, Fernando et al. 2022). According to recent studies, migration to urban regions and impervious surfaces substantially increase in next decade which considerable amount of land features will be replaced by urban areas (Qi, Ma et al. 2021). Flooding considered as the one of the most dangerous hazards due to its severe impacts on human life and environment. The Kurdistan region of Iraq, like other parts of the world, significantly affected by flash floods in recent decade. Flood risk mapping and building vulnerable areas using efficient techniques significantly contribute in better understand the flood patterns and providing insights for better decision making processes and mitigation planning strategies in densely populated areas (Membele, Naidu et al. 2022). Rapid urbanization and change in land use and hydrological conditions are the considerable factors impacting the flood intensities, especially in a city like Erbil, which faced multiple flood events in recent years. The land use pattern and replacing vegetated areas with impervious surfaces results in increased runoff and reduced natural drainage, which leads to more intense flood events, especially in urbanized areas with high population density (Ozkan and Tarhan 2016, Li, Zheng et al. 2023). The sustainable integration approaches play significant role in risk mitigation such as increased urban green spaces. The sustainable urban planning and disaster preparedness measures ensures the safety of infrastructures and human life. Building vulnerability assessment provides valuable insights for urban planners and disaster preparedness strategies.

The geospatial and remote sensing techniques offer valuable tools to assess the vulnerable areas, offering significant insights about flood risk areas that need mitigation strategies for urban planners. Moreover, integrating the geographic information system (GIS) with the Analytical Hierarchy Process (AHP) provides comprehensive approach to better understand and analyse the multiple and complex factors impacting the flood hazards, facilitating the decision-making processes (Iliadis, Galiatsatou et al. 2023). The diverse topography and rainfall patterns of Erbil city, which is the most populated city in Kurdistan region of Iraq, made the city to face severe challenges due to frequent floods in recent years. Erbil city faced substantial increase in urbanization and population, and with its unsuitable drainage system and decreased green spaces, the region affected by flood events in major parts of the city (Sarmah and Das 2018). The floods in 2018, 2020 and 2024 caused substantial economic loss, loss of life and infrastructure damages, indicating the need of rapid flood hazard analyses to understand the flood factors and mitigate its affects (Aziz, Saleh et al. 2023). Recent floods in Erbil city, in 2021 and 2022 killed 14 people and 55 were injured (K Sissakian, Al-Ansari et al. 2022). In some parts of the city flood covered homes with two meters (Aziz, Saleh et al. 2023).

Several researches have been implemented for flood hazard analysis sing different measures. Multiple studies used AHP integration with GIS techniques for Ranya city (Chomani 2023), Akre district (Fatah and Mustafa 2022), Mergasor (Mikail and Hamad 2023), Erbil Sub-Basin (Al–Shwani, Saleh et al. 2025) and Duhok city (M Amen, Mustafa et al. 2023) and analysed the flood hazards comprehensively. Moreover, HEC-RAS were used in different researches for Zerin City (Dawood and Mawlood 2023), Koya city (Dawood, Mawlood et al. 2021), Barzan area (Mustafa, Faisal et al. 2025), and Erbil city (Mustafa, Szydłowski et al. 2023). However, Decision Table Classifier and Metaheuristic Algorithms were used to assess the flood hazards in Sulaymaniyah (Askar, Zeraat Peyma et al. 2022) and another study integrated GIS with morphometric analysis to investigate the flood hazards in Gulasur Basin in Sulaymaniyah (Ibrahim 2021). Additionally, studies used the Storm Water Management Model (SWMM) approach in Erbil City to simulate the urban flood and assessing flood potential zones (Ali and

Mawlood 2023, Ali and Mawlood 2023). Moreover, the topographic wetness index (TWI) tool were integrated with Multi-Criteria Decision-Making in another study for Erbil basin to identify areas Exposed to Potential Flash Floods (Thannoun and Ismaeel 2024).

Having accurate mapping of flooded areas and generating flood susceptible regions ensures better decision making and can be used for disaster management and mitigation planning by policy makers. Recently, using the GIS, remote sensing and AHP integration critically facilitated the flood hazard analysis, resulting in better understanding the flood events and reducing its impacts on the peoples life and environment (Akhtar, Sajjad et al. 2023). The literature commonly used multi criteria decision-making (MCDM) as one of the effective approaches for flood assessment. Moreover, the analytical hierarchy process (AHP) used as the popular choice for considering multiple factors of flood events (Diaconu, Costache et al. 2021, Kaya and Derin 2023).

The building vulnerability assessment and flood hazard analysis in Erbil city by integrating the GIS, remote sensing and AHP techniques are the objective of this study. The study highlights the significance of building vulnerability mapping for disaster preparedness and more effective decision making process. Moreover, the results of the research significantly contribute in early warning system measures, providing effective tools to mitigate the flood risks to human lives, infrastructure, and economic activities.

2. Materials and methods

2.1. Study area

Erbil is the capital and the biggest town of Iraq's Kurdistan region, which has been continuously inhabited for around 6000 years and considered as one of the oldest settlements on earth by UNESCO World Heritage Site (Chomani 2024). The city witnessed multiple intense floods in recent years with severe damages. The rapid urbanization duo to economic stability after 2003 altered the land use pattern and hydrological conditions in the city, leading in more flood events. Three outlets were used to generate study area that covers entire urban region in Erbil city with 909 km2 (Fig. 1). The boundaries of the study area range from 393,022.85 m to 433,750.49 m in easting, while the northing boundaries extend from 3,994,865.63 m to 4,020,623.00 m, based on UTM coordinates (WGS 1984 Zone 38N). Having semi-arid weather, maximum rainfall intensity reaching 103 mm/day and insufficient drainage system makes the city highly prone to flood events, specifically during intense rainfall events.

There were several recent flood events in the Tayrawa which caused car damages and covering multiple buildings in the neighborhood, such as floods at 26-Nov-2018, 13-Jan-2022, 19-Mar-2023, 20-Nov-2023, and 3-May-2024 (www.kurdiu.org). The heavy rainfall in April 2024, caused floods in different parts in Erbil city, which inundated more than 50 houses and damaged more than 30 shops only in the Tairawa Bazar, which caused a blockage and led to the closure of transportation of the 30 meter street in Tairawa neighborhood. Moreover, two of the most significant flood events were from 2018 and 2021, which caused severe damages in the Erbil city. The flood event from 2021 resulted in damaging nearly 1189 cars, 408 houses, 350 local shop, and covering 3183 buildings in the Roshnbiry neighborhood. The flood caused 13 fatalities and 21 billion Iraqi Dinar economic damages (K Sissakian, Al-Ansari et al. 2022). The increased runoff coefficient due to urban development which increase the flood hazards as natural drainage systems are overwhelmed during heavy rains along with the inadequate drainage system and urban planning in Erbil city were identified as the primary contributors of flood events (K Sissakian, Al-Ansari et al. 2022, Aziz, Saleh et al. 2023, Mustafa, Szydłowski et al. 2023). Reports highlighted the damages of multiple sectors, including the residential, commercial and industrial areas. The most vulnerable regions were those which witnessed rapid urbanization (Aziz, Saleh et al. 2023).

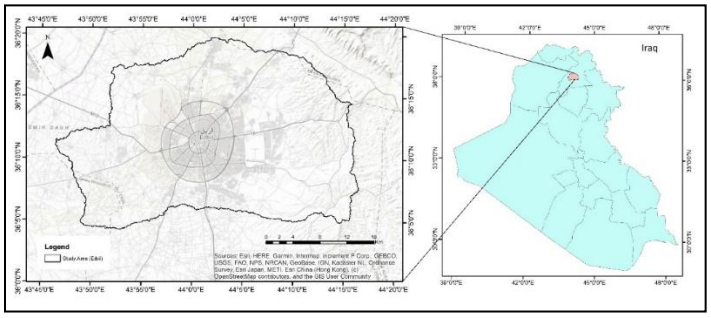

Figure 1: Study area with 908 km2 (Erbil city).

2.2. Dataset

Conditions of the topography, environmental criteria, the formation of geology, and anthropogenic conditions of the study area were significant factors contributed to flood events. Alaska Satellite Facility (ASF) were used for acquiring a pre-processed digital elevation model (DEM) with 12.5 m resolution from ALOS PALSAR satellite. Flow accumulation, slope, aspect, TWI , SPI, drainage density and elevation were generated using DEM. Soil map from Ministry of Agriculture in Bagdad were utilized to generate soil data for the study area. Lithology map for Erbil city has been created using FAO dataset (Stevanovic 2003). Moreover, the rainfall data were collected from the General Directorate of Meteorology and Seismology in Erbil between 2003 and 2023. Additionally, the land use land cover (LULC) and road map for were created using Planet's SuperDove and NDVI, NDBI were generated from sentinel 2 imagery. The population data from previous studies were used and the estimated population for 2023 for Erbil city were generated using exponential growth projection. The datasets and their sources were mentioned in Table 1.

Table 1: The characteristics of the utilized dataset in this research.

Datasets	Date	Resolution	Generated thematic maps	Source
Planet (SuperDove) imagery	6, April, 2023	Ground sample distance: 3.7 m Coastal Blue Blue Green I Green II Yellow Red Red Edge Near Infrared (NIR)	Land use land cover Road proximity NDVI	https://planet.com/
Sentinel 2 imagery	6, April, 2023	Red, NIR: 10 m SWIR: 20 m	NDBI	https://developers.google.com/earth-engine/datasets/
DEM	2006 - 2011	12.5 m	Slope, aspect, flow accumulation, TWI, SPI, drainage Density	https://asf.alaska.edu/
Lithology map	2003	Raster image	Lithology map	FAO (Stevanovic 2003)
Soil data	1957	Raster image	Soil map	Ministry of agriculture, Bagdad. (Buringh 1957)
Rainfall	2023	Daily data	Rainfall map	The General Directorate of Agriculture in Erbil, Kurdistan Region of Iraq.
Building footprint database	2023 - 2024	Up to 10 meter	Building footprint map for Erbil city	Microsoft: https://planetarycomputer.microsoft.com/dataset/ms-buildings, OpenStreetMap: https://data.humdata.org/dataset/hotosm

				_irq_buildings
Historical flood records	2003-2023	-	Historical flood map	Sentinel 1 imagery and Civil Defense Directorate of Erbil Governorate, local news and field trips.
Population data	2000 – 2020	-	Population density	(Ismael, 2024)

2.3. Methodology and Flood vulnerability factors

Methodology of this research basically depended on assigning 14 parameters based on their impact on flood events in Erbil city using expert opinions and the literature. Considered factors are such as normalized difference vegetation index (NDVI), drainage density (DD), elevation, stream power index (SPI), land use land cover (LULC), normalized difference built-up index (NDBI), flow accumulation (FA), lithology (L), soil data (SO), aspect (A), topographic wetness index (TWI), rainfall (R), slope (SL), and distance to roads (DR) for mapping flood susceptibility mapping in Erbil city. The Analytic Hierarchy Process (AHP) were employed as main methodology to weight assignments of each selected parameters, which is a structured techniques for organizing the complex decisions. The process of weighting the parameters were based on using pairwise comparison (PC) matrix, which expert opinions and contribution of the parameters on flood events in the study area were used to calculated the weights of the factors. The Saaty's scale of 1 to 9 were employed to compare the factors, where 1 means equal importance and 9 indicates extreme importance of one factor over another (Saaty and Vargas 2012). The flowchart and process of the study were illustrated in figure 2. These 14 factors (Figure 3) can be considered as the significant parameters have impact on the flood events with different degree according to the relevant studies (Table 2).

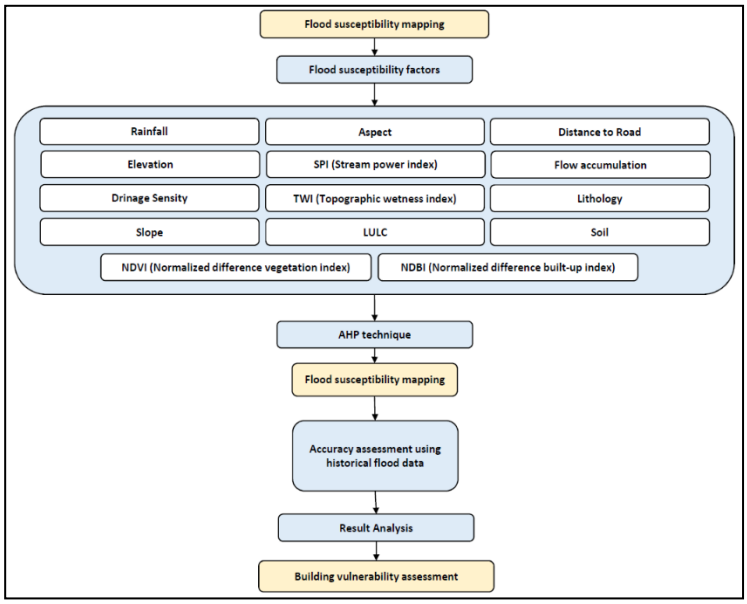

Figure 2: Flowchart of the building vulnerability mapping.

2.3.1. Drainage Density (DD)

One of the most significant factor which plays significant role in behaviour of water, is the natural drainage lines. The drainage density is one of the significant parameters which commonly used by different studies for FSM. The DD for this study created using the process of flow accumulation and flow direction from digital elevation model utilizing the ArcGIS Pro 3.3 geoprocessing tools. The DEM data pre-processed and cleaned from the sinks to ensure the correct hydrological surfaces in the region (Dwivedi, Pandey et al. 2022). Following this, the direction of water flow across the landscape was determined using the flow direction tool and utilized to generate the drainage network. Additionally the total length of streams were calculated using flow accumulation (Das and Pardeshi 2018). Total length of the drainage network was divided by the area of the watershed to generated DD (Lin, Pan et al. 2021). The higher value of DD tends to increase the

flood susceptibility, as is shows the channels water capacity (Talha, Maanan et al. 2019, Al-Sababhah 2023). The DD was classified into 5 different categories ranging from 1 to 5. The PC matrix defined the weight of DD as 12%.

2.3.2. Slope (SL)

The slope is a significant factor that contribute in accumulation of water and floods. Multiple studies identifies the slope as one of the main parameters that should be used for FSM. Areas with small slopes lead to slower runoff and more inundation, resulting in increasing the susceptibility to flooding compared to steeper terrains (Ibeabuchi 2023, MAGUREANU, Sfîrcoci et al. 2023). The thematic map of slope was generated from digital elevation model using ArcGIS Pro slope tool. The thematic map of slope is classified into four different classes, the lower slopes ranked highest contribution with 5, and the slopes with more than 30 degree was assigned as least possibility of flood. The weight of the slope was 11% based of pairwise comparison (PC) matrix.

2.3.3. Rainfall (R)

One of the commonly used parameter for FSM is the rainfall map, which have critical impact on the flood hazards. Studies showed that the integration of AHP and GIS provides systematic evaluation of multiple complex parameters to generate comprehensive flood vulnerability maps (Allafta and Opp 2021, Desalegn and Mulu 2021, Bui, Luu et al. 2023). The rainfall data from 4 different meteorological stations in Erbil governorate were collected for 2023 from the General Directorate of Agriculture in Erbil, Kurdistan Region of Iraq. The Kriging tool from ArcGIS Pro was used to interpolation the points and the rainfall map was generated (Panday, Maharjan et al. 2018). The map was classified into 5 classes, the class with highest rainfall was ranked as 5 and the lowest as 1, considering their influence on flood hazards.

2.3.4. Land use land cover (LULC)

The LULC plays a critical role in identifying areas prone to flooding, as it affects hydrological and runoff characteristics within a watershed. The Land Use Land Cover (LULC) imagery for the study area was created using Planet's SuperDove satellite imagery with three different classes: Built-up area, vegetation and barren land. The support vector machine (SVM) algorithm from ArcGIS Pro 3.3 was used to generate the LULC map, as it showed superior performance over other machine learning techniques in different applications (Mushtaq, Mahmood et al. 2021, Chomani and Pshdari 2024). SVM is a popular and powerful classifier used for LULC mapping due to its effectiveness in handling high-dimensional data and non-linear relationships, which is based on constructing hyperplanes in a multidimensional space to optimally separate different classes of land cover, leading to accurate identification of the land features (Ibrahim Mahmoud, Duker et al. 2016, Bouaziz, Eisold et al. 2017). The built-up area was ranked as 5, as the urban regions most vulnerable to floods due to increased impervious surfaces, while the green areas ranked as 1 (Al-Sababhah 2023). The overall weight of the LULC was identified by PC as 9%.

2.3.5. Topographic wetness index (TWI)

The Topographic Wetness Index (TWI) is considered as an indicator of hydrological characteristics by determining the potential for water accumulation based on terrain characteristics, which is essential for understanding flood risks in various landscapes (Mujib, Apriyanto et al. 2021). Using TWI (eq. 1)(Thannoun and Ismaeel 2024) with AHP and GIS technology enhances spatial analysis capabilities, aiding in more accurate identification of flood-prone areas (Cabrera and Lee 2019, Yagoub, Alsereidi et al. 2020). The 12.5 meter DEM and ArcGIS Pro tools were used to generate the TWI map and the classes were ranked based on their contribution on the flood hazard risks.

$$TWI = \ln\left(\frac{catchment\ of\ the\ area}{\tan(slope)}\right) \quad (1)$$

Where the catchment of the area is in m2.

2.3.6. Elevation (E)

Elevation is another factor which can contribute in flood vulnerable regions. Regions with lower elevation are generally more prone to flooding compared to those at higher altitudes (Hoque, Tasfia et al. 2019, Desalegn and Mulu 2021). The elevation map for this study created from

DEM, which was downloaded from ALOS PALSAR satellite with 12.5 m resolution. Moreover, the accuracy of elevation map significantly influence the results of FSM (Ullah and Zhang 2020, Adedoja, Popoola et al. 2023). The study area elevations ranged from 315 to 1107, which classified into 5 classes ranking from 1 to 5 with overall weight of 7% based on PC.

2.3.7. Distance to roads (DR)

The historical flood events indicated that there are multiple flood events in the main roads in Erbil city. Using the map of road proximity plays an essential indicator in flood vulnerability, as areas closer to major roads are more susceptible due to increased human activity and infrastructure density (Osman and Das 2023). Additionally, studies highlighted that the proximity of urban areas to roads have a significant correlation with flood risk (Zia, Shirazi et al. 2021). The SuperDove Planet imagery from 2023 was used to digitize the main streets in Erbil city manually, and the Euclidean Distance Spatial Analyst tool from ArcGIS Pro was used to generate road proximity map, which classified into four different categories (Johnston, Ver Hoef et al. 2001). Regions with more proximity with roads was ranked as highest influence on flood hazards and vice versa.

2.3.8. Normalized Difference Vegetation index (NDVI)

The integration of the Normalized Difference Vegetation Index (NDVI) provides significant insights related to the vegetation conditions, which have critical contribution in flood dynamics by affecting the runoff conditions. Areas with low value of NDVI tend to have more vulnerability to flooding due to reduced vegetation cover (Ullah and Zhang 2020, Khaldi, Elabed et al. 2023, Mukhtar, Shangguan et al. 2024). Using NDVI (eq. 2)(D'Allestro and Parente 2015) with other flood contributed factors, aid in enhancing the accuracy and reliability of FSM. The near infrared and red bands of SuperDove satellite imagery form April, 2023 were used to generate the NDVI map for the study area with values from -1 to 1. The generated map of NDVI, reclassified into four classes using ArcGIS Pro. Moreover, the NDVI weight was assigned as 6% based on PC matrix.

$$\mathrm{NDVI} = \frac{(\text{Near infrared} - \text{Red})}{(\text{Near infrared} + \text{Red})} \quad (2)$$

2.3.9. Stream power index (SPI)

The Stream Power Index (SPI) used as a factor for generating FSM. The SPI quantifies the potential energy available for sediment transport in a river system, which aid significantly for better understanding the dynamics of flood (M Amen, Mustafa et al. 2023, Al-Omari, Shatnawi et al. 2024, Kara and Singh 2024). The SPI thematic map was created using DEM from ArcGIS Pro and the result classified into 5 different classes. The higher SPI (eq. 3) value was assigned with ranking 5, which means most influence on flood, and lowest values assigned as 1, indicating the low effect on flood hazards.

$$\mathrm{SPI} = Area\ \mathrm{of}\ catchment\ * \tan(slope) \quad (3)$$

Where the catchment of the area is in m2 and the slope is in degree.

2.3.10. Normalized difference built-up index (NDBI)

The Normalized Difference Built-up Index (NDBI) is an index for distinguishing built-up from non-built-up regions which is based on short-wave infrared and near-infrared bands. It is an effective factor to evaluating the impact of urbanization on flood vulnerability (Ghosh, Mandal et al. 2018, Azizah, Deffinika et al. 2022). The value of NDBI is between -1 to 1. The lower value indicates the non-buildup areas, which the values near to 1 are urbanized regions. NDBI (eq. 4) created from the Sentinel 2 satellite imagery using both shortwave infrared and near infrared bands and the map classified into 4 different classes with ranking from 1 to 5, built up regions assigns as ranking 5 and non-built up regions ranked as 1 in flood contribution. The regions with more possibility of urban areas assigned with ranking 5 and non-urban regions with 1. The PC matrix calculated the weight of NDBI as 5%.

$$\mathrm{NDBI} = \frac{(\text{Shortwave infrared} - \text{NIR})}{(\text{Shortwave infrared} + \text{NIR})} \quad (4)$$

2.3.11. Lithology (L)

Lithology is another critical factor that have influence on the soil permeability and runoff characteristics. Permeable soils tend to have more infiltration rates, while impermeable lithological formations increase the flood probability due to limited infiltration (Zzaman, Nowreen et al. 2021, Megahed, Abdo et al. 2023).

The lithology map has been digitized using digital imagery from FAO dataset for the study area using ArcGIS Pro (Stevanovic 2003). The study area consisted of four types of lithological formations, such as River Terraces, Muqdadiya Formation, Injana Formation, and Bai Hassan Formation. Using lithology map as a factor for flood susceptibility mapping enhance the accuracy and reliability of the flood hazard assessments.

2.3.12. Soil data (SO)

Using soil maps as a parameter with integration of the Analytic Hierarchy Process (AHP) and Geographic Information Systems (GIS) is a significant approach for generating reliable flood vulnerability mapping. Soil type have a critical impact on hydrological processes, including infiltration rates and runoff potential, which are significant for better understanding the behavior of flood hazards (Dano, Balogun et al. 2019, Desalegn and Mulu 2021). Studies indicated the soil characteristics, such as moisture retention and permeability, are critical for in flood susceptibility determination (Talha, Maanan et al. 2019). The soil map was digitized and thematic map was generated for the study area using soil dataset from Ministry of agriculture in Bagdad (Buringh 1957). The study area was consisted of three different types of soils, which ranked based on the impact on the flood events.

2.3.13.Aspect (A)

Aspect is one of the critical parameters which enhance the accuracy of flood vulnerability mapping, as it has a significant role in determining how water flows over a landscape and vegetation growth and soil moisture levels. Aspect shows the direction of land surfaces face, which significantly impact the water flow and accumulation. Aspect indicate how topography affects hydrological processes, providing valuable insights for determining areas at risk of flooding (Manfreda, Samela et al. 2018, Hariyono and Kurniawan 2022). The aspect map was created from DEM using ArcGIS Pro tools and the generated map was ranked from 1 to 5 based on their influence on the flood hazards.

2.3.14.Flow accumulation (FA)

It has been approved recently that the flow accumulation conducted as a significant factor for mapping flood hazards, which is based on quantifying the potential for water accumulation based on topography and hydrological conditions (Vojtek and Vojteková 2019, Khoeun, Sok et al. 2022, Eryani, Jayantari et al. 2024). The flow accumulation was created from the DEM using ArcGIS Pro tools, and the thematic map categories were generated into 5 categories. After removing the sinks in DEM using fill tool, the flow direction was determined for each cell which is based on the steepest descent (Staponites, Barták et al. 2019). Finally the flow direction raster used to calculate flow accumulation which sums the number of cells that contribute flow to each cell (Celone, Pecor et al. 2022). The regions with more flow accumulation tend to have more influence on flood events compared to low flow accumulation.

Table 2: Relevant factors used in the flood susceptibility mapping in various studies.

Reference	SP	EI	R	A	TWI	FA	LULC	DD	LT	SO	SPI	DR	NDVI	NDBI
(Mikail and Hamad 2023)	x	x	x	x			x	x	x	x		x	x	
(Askar, Zeraat Peyma et al. 2022)	x	x	x		x		x		x		x		x	
(Mustafa, Szydłowski et al. 2023)		x	x				x			x				
(Chomani 2023)	x	x	x	x	x		x	x			x	x		
(Fatah and Mustafa 2022)	x	x	x		x	x	x	x	x	x	x		x	
(Nguyen, Fukuda et al. 2024)	x	x	x		x		x	x				x	x	
(Mech	x	x	x		x		x		x			x		x

entel, Dairi et al. 2024)													
(Ray 2024)	x		x		x		x	x	x	x			x	x
(Mohar rir, Singh et al. 2024)	x	x			x		x	x		x				
(Shivh are, Kuma r et al. 2024)	x	x	x		x		x	x			x	x	x	
(Khad dari, Jari et al. 2023)	x	x	x			x	x		x					
(Abrar , Iman et al. 2024)	x	x	x		x		x	x		x		x	x	
(Mokh tari, Abdel kebir et al. 2024)	x	x	x		x			x	x				x	
(Diriba, Takele et al. 2024)	x	x	x				x	x		x				
(Huu Duy, Tuan Pham et al. 2024)	x	x	x	x	x		x			x		x	x	x

Table 3: The pairwise comparison matric with weights (W) of all 14 factors.

Factors	SL	E	R	LULC	DD	TWI	L	SO	A	SPI	NDVI	NDBI	DR	FA	%W
SL	1	1	1	2	0.5	2	2	2	2	2	3	2	1	4	11
E		1	1	1	0.5	1	1	2	2	2	1	2	1	1	7
R			1	2	0.5	2	2	2	2	2	2	2	2	2	10
LULC				1	0.5	1	3	2	2	2	2	2	1	2	9
DD					1	1	2	2	2	3	3	2	1	3	12
TWI						1	1	1	2	2	2	2	1	3	8
L							1	1	1	1	1	1	1	1	5
SO								1	1	1	1	1	0.5	2	5
A									1	1	1	2	0.5	2	5
SPI										1	1	2	0.5	3	6
NDVI											1	2	1	3	6
NDBI												1	1	3	5
DR													1	2	7
FA														1	4

The contribution of all the conducted 14 parameters in the flood susceptibility mapping can be seen below in figure 3

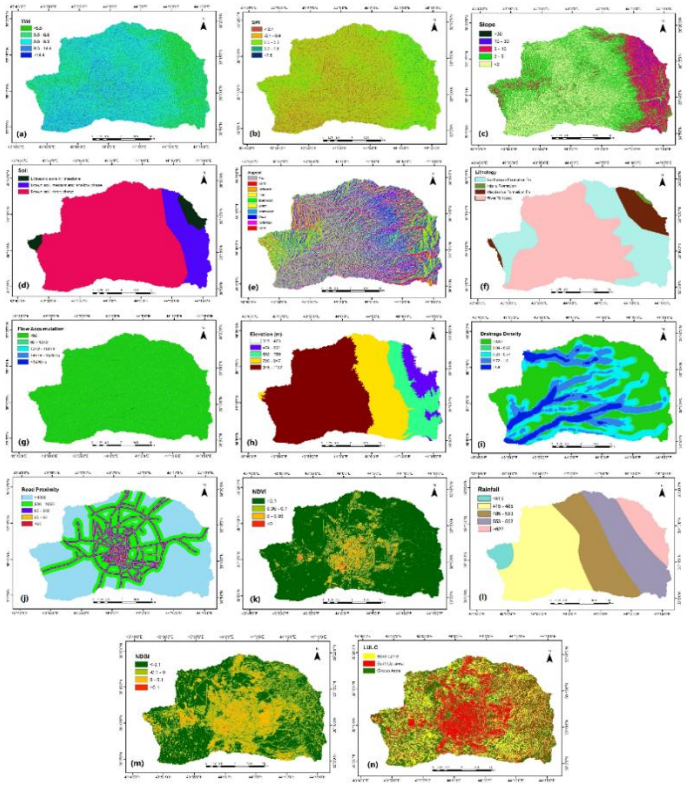

Figure 3: The contributed factors for flood susceptibility mapping, including: (a) TWI, (b) SPI, (c) Slope, (d) Soil, Aspect (e) , (f) Lithology, (g) Flow accumulation, (h) Elevation, (i) Drainage density, (j) Road proximity, (k) NDVI, (l) Rainfall, (m) NDBI, and (n) LULC.

2.4. Analytic Hierarchy Process (AHP)

AHP is the most commonly used approach of multi criteria decision-making process (MCDP) for flood hazard analysis, which considers complex factors together to identify flood susceptible areas with reliable accuracy (Membele, Naidu et al. 2022, Kaya and Derin 2023). AHP is a structured decision-making approach which is designed to make complex decisions by breaking them down into simpler components. AHP process is based on organizing parameters into a hierarchical structure, allowing decision-makers to perform pairwise comparisons (PC) and determining their relative importance (Benítez, Delgado-Galván et al. 2012, Mishra, Pundir et al. 2017). The PC were used to assign weights of factors contributed to floods considering their impact. The AHP calculation were performed using ArcGIS pro 3.3. Interestingly, the matrix of pairwise comparison (PC) were used along with expert opinion to evaluate and ranking the parameters, the flood risk areas were identified for Erbil city considering the 14 flood related factors integrating the AHP technique. Table 3 and 4 gives information related to the weights of each parameters and rankings of each classes of different criteria. The reliability of PC matrix were performed using consistency ratio (CR), which should be less than 10% (Saaty and Vargas 2012). The assessment showed acceptable CR value with only 4.3%. The support vector machine (SVM) as one of the effective classifiers from ArcGIS Pro 3.3 was used for generating the LULC map using high resolution Planet satellite imagery with three classes: Barren land, vegetated area, settlement area. The formula of kappa coefficient (KC) (Chomani and Manguri 2024) were utilized with 100 random point to calculate the accuracy of the generated LULC. The result showed that the accuracy of classified image with 84%, indicating the high performance and accuracy of the SVM algorithm (Table 5).

Table 4: The rankings and weights of each 14 parameters used in FSM (W: weight; R: ranking).

Factors	Sub-classes	W (%)	R	Factors	Classes	W (%)	R
Flow accumulation (FA)	Less than 92	4	1	Rainfall (RF)	Less than 415	10	1
	92 to 1242		2		415 - 485		2
	1242 to 15514		3		485 - 553		3
	14414 to 192615		4		553 - 622		4
	More than 192615		5		More than 622		5
Soil (SO)	Deep phase, Brown soil	5	5	NDBI	Less than -0.1	5	1
	Medium and shallow Brown soils, phase over bakhtiary gravel		4		-0.1 to 0		2
	Lithosolic soils in limestone		3		0 to 0.1		4
					More than 0.1		5
Lithology (LY)	River Terraces	5	5	NDVI	-0.17 to 0	6	5
	Muqdadiya Formation (Fn.)		4		0 to 0.05		3
	Injana Formation (Fn.)		3		0.05 to 0.1		2
	Bai Hassan Formation (Fn.)		2		0.1 to 0.23		1
Elevation (EL)	315 to 473	7	5	Slope (SL)	0 to 2	11	5
	473 to 631		4		2 to 5		4
	631 to 789		3		5 to 15		3
	789 to 947		2		15 to 30		2
	948 to 1107		1		More than 30		0
Distance to Road (DR)	Less than 20	7	5	LULC	Built-up area	9	5
	20 - 60		4		Vegetation		1
	60 - 200		3		Barren land		3
	200 - 1000		2	SPI	-5.3 to -2.1	6	1
	More than 1000		1		-2.1 to 0.9		2
TWI	3 to 5.5	8	1		0.9 to 3.3		3
	5.5 to 6.8		2		3.3 to 7.8		4
	6.8 to 9.3		3		7.8 to 14.3		5
	9.3 to 14.4		4	Aspect (A)	Flat	5	5
	More than 14.4		5		Northwest		4
Drainage Density (DD)	Less than 0.09	12	1		North		4
	0.09 to 0.29		2		West		3
	0.29 to 0.77		3		Northeast		4
	0.77 to 1.9		4		East		3
	More than 1.9		5		Southwest		2
					Southeast		2
					South		1

Table 5. The kappa matrix classification (Kohen 1960).

Kappa classes	Categorization
< 0.2	Poor
0.210 − 0.4	Fair
0.410 − 0.6	Medium
0.610 − 0.8	Good
> 0.80	Very Good

2.5. Flood susceptibility mapping using AHP technique

Having accurate mapping of flood risk areas using AHP technique, provides valuable insights to better understand the flood patterns, which significantly contribute in mitigation strategies and early warning system development. By considering all 14 factors using AHP approach, we identified vulnerable areas to floods in four different categories: very high, high, medium and low. Moreover, the overlay analysis were performed to the result of flood prone areas to identify the building vulnerability to floods using the integrated datasets of Microsoft and OpenStreetMap building footprints. Both datasets were combined to fill the gaps and enhance the reliability of the dataset. The flood susceptibility maps were utilized to identify the exact location and number of buildings that are at risk of floods in Erbil city, which can be used effectively for early warning system development by officials and to mitigate the severe impacts of floods on residents and infrastructures.

3. Results and Discussions:

3.1. Flood susceptibility mapping

AHP technique is one of the popular and effective approach which facilitate the complex relationship between multiple factors, which can be used to accurate mapping of flood prone areas using the integration of GIS and remote sensing techniques. The flood susceptibility maps (FSM) were created for the Erbil city with very high, high, medium and low flood risk areas. The diverse distribution of vulnerability were revealed by the flood hazard assessment. The majority of the areas were under low risk category with 555 km² (61.1%), showing that the area are relatively safe to flood events (Figure 4). A significant part of the total area, 245 km² (27%), were identified as medium risk class, indicating it as a moderate flood prone area. Additionally, the results showed that 3.9% (35 km2) and 8.2% (74 km2) of Erbil city were located in very high and high flood risk zones, respectively (Table 6). Moreover, the results of spatial distribution (Figure 4) indicated a notable pattern of flood risk areas, showing that high and very high risk areas were located in urban regions in center and south east of the city, emphasizing the vulnerability of highly populated areas to flooding. However, low and moderate risk categories were specifically located in barren land outside of the urban regions, highlighting the less populated regions face lower flood events (Fig. 4, a). This complex relationship between urbanized areas, LULC and flood risk, stressing the importance of implementing flood mitigation measures significantly considering these related factors, specifically in urban areas.

Table 6: Statistics of generated FSM for four classes.

Flood risk categories	Area (km2)	%
Low	555	61.1
Medium	245	27
High	74	8.2
Very High	35	3.9

Having accurate maps of flood vulnerable regions, offers significant insights for officials to better analyse the flood patterns and implement mitigations strategies to reduce the flood hazard impacts. Field trips, local news, historical flood events in the Civil Defense Directorate of Erbil Governorate in Erbil, and sentinel 1 imagery were integrated together to generate past flooded location to assess the accuracy of FSM results generated by AHP. The Area under the Receiver Operating Characteristic (AUC-ROC) curve is a significant approach for evaluating the performance of results of FSM. AUC-ROC is based on the plotting the true positive rate against the false positive rate at various threshold settings, to visualize the trade-offs between specificity and sensitivity in the generated results (Klingenstein, Haritoglou et al. 2011, Chen and Samuelson 2014). The AUC determines the overall accuracy of the results with values ranging from (indicating no ability to

discriminate) to 1.0 (flawless discrimination), offering an effective predictive power of the model (Jiménez-Valverde 2012). 41 historical points were collected and were compared with FSM of very high risk zones. The accuracy assessment indicated that 37 out of 40 (92.5%) of points were located in high and very high flood susceptible areas, and the accuracy of the map was 92.2% using AUC-ROC curve (Figure 5), indicating the high accuracy of generated flood vulnerability map using AHP approach.

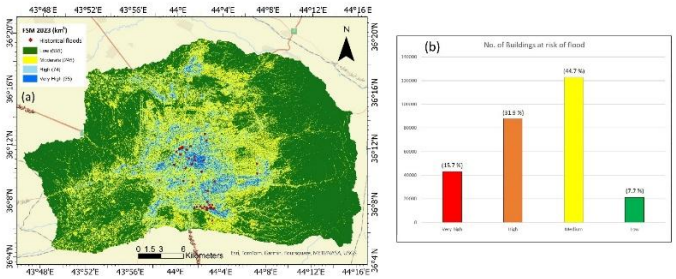

Figure 4: Flood susceptibility map of Erbil city using AHP (a) and number of Buildings Vulnerable to Flooding with four categories: Very high, high, medium and low risk (b).

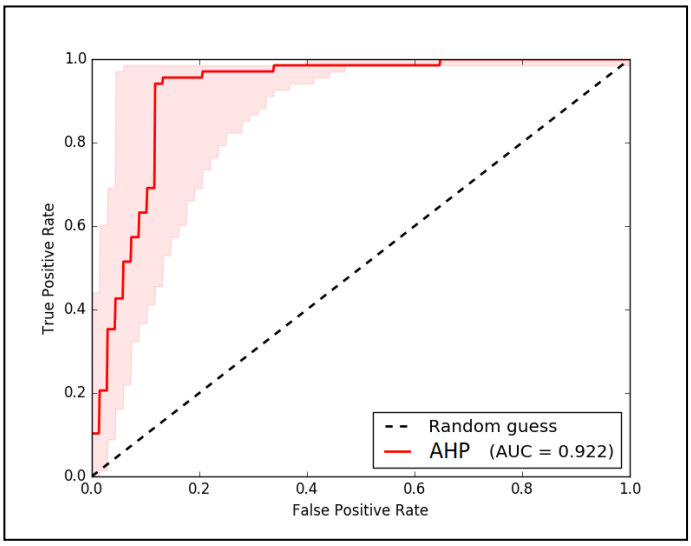

Figure 5: AUC value and ROC curve for generated FSM.

3.2. Susceptibility Analysis of Environmental and Topographic Parameters

The flood hazard analysis were performed for various environmental and topographic parameters to examine the distribution of each parameter across the different flood susceptibility zones. The results emphasised notable variations in spatial distribution of each actor, highlighting the significant role of the contributed factors in identifying regions vulnerable to flood. The distribution of the parameters across the flood hazard levels (low, medium, high and very high) were presented in detail in Table 7. The results of flow accumulation parameter showed that the majority of the area falls under the “Low” category, covering 59.36% of the total area. Moreover, the percentage of the area decline as the value of flow accumulation increases. Only 0.15% of the area were in very high flood susceptibility category. Regarding the soil types, the Deep phase, Brown soil class were the dominant one by covering the 42.86% of the low flood category. However, the representation of other soil types such as Medium and shallow Brown soils over Bakhtiary gravel and Lithosolic soils in limestone were minimal across all hazard levels, specifically in higher categories. Moreover, the analysis indicated that the most prominent lithological formations were the River Terraces and Bai Hassan Formation, which contributed notable portion of the areas from all the hazard levels in the study area. On the other hand, very limited presence, specifically in higher hazard categories, were noted from the lithological formations such as Muqdadiya and Injana Formation. Regarding the Elevation factor, the results highlighted that the area with most coverage was located between elevation of 315 and 473 meters, which accounted for 26.49% of the low flood hazard category. As expected, the higher elevation regions were rare across all hazard categories. Additionally, the results of distance to road indicated its significance and contribution on flood hazards. Large portion of the area (42.45%) which is 1000 meters away from the roads, were distributed on low hazard category, and the more road proximity were decreased, the percentage in hazard categories also decreased.

Furthermore, for TWI, the results indicated that values ranging from 3 to 5.5 dominated the low flood hazard category, which covered 16.06% of the study area. Notably, the higher wetness levels, such as values greater than 14.4, were distributed and have more presence in very high flood hazard category, indicating that these areas

are more prone to flood hazards. When considering the drainage density, the results showed that areas with very low drainage density with values less than 0.09, covered significant portion of the low hazard category with 33.56%. In contrast, the higher drainage density areas with values more than 1.9, were found more commonly in high and very high flood hazard categories, indicating the significant contribution and correlation between drainage systems and flood hazards. Additionally, rainfall plays notable role, which values ranging from 415 to 485 mm represented 21.04% of the areas of low flood hazard category, while the higher values represented minimal portions in higher categories. The outcome of the NDBI showed that values less than 0.1 dominated 40.26% of the low category, indicating the large portion of non-urbanized areas in the study area. However, the higher values of NDBI showed minimum presence in the very high category. Moreover, regarding the NDVI results, the results showed that the values ranging from 0.1 to 0.23 were the highest portion of area in lower flood risk regions with 59.12%. Conversely, the higher values were noted in higher hazard categories with small proportion of coverage. In terms of slope, the majority of the land were covered with gentle slopes with less than 5 degrees, which covered a large portion of the areas with low flood hazard category with 41.74%. Also the results showed that the steeper slopes with greater than 15 degrees, showed minimal presence in the higher hazard levels, which indicated the minimal influence of the steeper slopes in flood risks. Moreover, the analysis of LULC showed that the built-up areas are more presented in the medium and high hazard categories, showing the significant of the developed areas in flood events. Conversely, the low hazard category were dominated by the vegetated and barren land features, highlighting the significant role of the natural land features in reducing the flood risk. Lastly, the SPI results showed that lower values ranging from 0.9 to 3.3 dominated 34.6% of the areas in low category. However, higher SPI values (above 7.8) showed more presence in high and very high hazard categories, highlighting that regions with higher stream power are more prone to flooding.

Table 7: Distribution of each parameters across flood susceptibility classes in the study area.

Factors	Ranking of the	Flood susceptibility category (km2)							
		Low	%	Medium	%	High	%	Very high	%
Flow accumulation	1	539.01	59.36	222.98	24.56	64.62	7.12	22.67	2.50
	2	12.85	1.41	14.63	1.61	5.60	0.62	6.09	0.67
	3	3.16	0.35	5.31	0.59	1.94	0.21	2.62	0.29
	4	0.17	0.02	1.54	0.17	1.25	0.14	2.26	0.25
	5	0.00	0.00	0.21	0.02	0.45	0.05	1.35	0.15
Soil	5	389.20	42.86	241.27	26.57	72.10	7.94	34.86	3.84
	4	133.26	14.68	4.35	0.48	0.24	0.03	0.09	0.01
	3	34.43	3.79	0.29	0.03	0.01	0.00	0.00	0.00
Lithology	5	222.28	24.48	201.47	22.19	70.14	7.72	34.20	3.77
	4	72.45	7.98	3.95	0.43	0.23	0.02	0.05	0.01
	3	4.22	0.47	0.02	0.00	0.00	0.00	0.00	0.00
	2	256.43	28.24	39.10	4.31	3.43	0.38	0.77	0.09
Elevation	5	240.51	26.49	155.05	17.08	56.52	6.22	28.89	3.18
	4	117.65	12.96	81.40	8.96	16.93	1.86	6.01	0.66
	3	126.08	13.89	7.10	0.78	0.36	0.04	0.08	0.01
	2	57.41	6.32	1.11	0.12	0.05	0.01	0.01	0.00
	1	13.55	1.49	0.01	0.00	0.00	0.00	0.00	0.00
Distance to Road	5	1.95	0.21	6.85	0.75	5.57	0.61	4.98	0.55
	4	5.07	0.56	13.68	1.51	8.77	0.97	6.05	0.67
	3	26.29	2.90	46.39	5.11	22.07	2.43	11.54	1.27
	2	136.45	15.03	108.08	11.90	30.32	3.34	10.62	1.17
	1	385.43	42.45	69.66	7.67	7.13	0.78	1.80	0.20
TWI	1	145.83	16.06	14.59	1.61	0.83	0.09	0.02	0.00
	2	197.86	21.79	69.68	7.67	12.27	1.35	1.19	0.13
	3	159.22	17.54	93.26	10.27	29.22	3.22	7.78	0.86

	4	51.07	5.62	60.68	6.68	27.84	3.07	18.79	2.07
	5	1.23	0.14	6.46	0.71	3.70	0.41	7.21	0.79
Drainage Density	1	304.73	33.56	53.23	5.86	8.14	0.90	1.74	0.19
	2	33.39	3.68	13.10	1.44	2.72	0.30	0.72	0.08
	3	124.33	13.69	70.46	7.76	18.99	2.09	7.09	0.78
	4	63.26	6.97	74.36	8.19	30.61	3.37	16.83	1.85
	5	29.48	3.25	33.51	3.69	13.41	1.48	8.62	0.95
Rainfall	1	29.06	3.20	0.80	0.09	0.04	0.00	0.01	0.00
	2	191.01	21.04	117.70	12.96	35.73	3.93	15.25	1.68
	3	81.74	9.00	84.40	9.30	32.35	3.56	18.01	1.98
	4	170.13	18.74	38.20	4.21	5.46	0.60	1.60	0.18
	5	83.45	9.19	3.52	0.39	0.20	0.02	0.05	0.01
NDBI	1	365.52	40.26	59.43	6.55	4.38	0.48	1.35	0.15
	2	138.16	15.22	108.47	11.95	34.80	3.83	15.75	1.73
	4	50.81	5.60	75.19	8.28	34.00	3.74	17.48	1.92
	5	0.71	0.08	1.55	0.17	0.67	0.07	0.38	0.04
NDVI	5	0.28	0.03	1.23	0.14	1.11	0.12	1.15	0.13
	3	2.38	0.26	24.05	2.65	20.16	2.22	13.26	1.46
	2	15.70	1.73	51.51	5.67	24.23	2.67	11.12	1.22
	1	536.84	59.12	167.85	18.49	28.36	3.12	9.44	1.04
Slope	5	129.69	14.28	126.65	13.95	51.87	5.71	30.64	3.37
	4	249.24	27.45	111.25	12.25	21.59	2.38	4.32	0.48
	3	159.25	17.54	6.71	0.74	0.40	0.04	0.03	0.00
	2	17.01	1.87	0.06	0.01	0.00	0.00	0.00	0.00
	0	0.01	0.00	0.00	0.00	0.00	0.00	0.00	0.00
LULC	5	93.79	10.33	120.23	13.24	56.78	6.25	29.76	3.28
	1	237.51	26.16	33.39	3.68	2.89	0.32	0.89	0.10
	3	223.86	24.65	91.01	10.02	14.18	1.56	4.32	0.48
SPI	1	25.16	2.77	25.91	2.85	13.40	1.48	5.81	0.64
	2	173.91	19.15	91.01	10.02	22.29	2.45	7.65	0.84
	3	314.13	34.60	105.10	11.57	29.34	3.23	11.52	1.27
	4	40.75	4.49	19.73	2.17	7.10	0.78	6.77	0.75
	5	1.25	0.14	2.92	0.32	1.72	0.19	3.24	0.36
Aspect	5	55.91	6.16	67.46	7.43	33.12	3.65	23.44	2.58
	4	147.96	16.29	58.45	6.44	16.98	1.87	5.55	0.61
	3	115.09	12.68	44.79	4.93	11.49	1.27	2.99	0.33
	2	156.15	17.20	52.81	5.82	9.89	1.09	2.45	0.27
	1	80.09	8.82	21.15	2.33	2.38	0.26	0.57	0.06

3.3. Buildings Vulnerable to Flooding

Building footprint maps from the combination of Microsoft and OpenStreetMap were used to achieve the overlay analysis with the FSM classes to identify the spatial distribution of buildings which are at risk of flood events in the study area. The four classes of flood risks were used to generate four classes of buildings as: very high, high, medium, and low risk buildings. There were 274735 building footprints in the study area, which the outcome showed that 43125 buildings (15.7%) were in very high risk regions of flooding. Moreover, the 87758 (31.9%), 122762 (44.7%), and 21090 (7.7%) buildings were identified in high, medium, and low risk regions. The results indicated that near the half of the buildings in Erbil city were highly susceptible to flood hazards, as identified in the outcome in high and very high flood risk regions with total 47.6% combined (Fig. 4, b). Additionally, the results showed that buildings in neighborhoods of Daratu in the south, Khabat in the east and Newroz neighborhoods were the most vulnerable to flooding. Figure 6 shows the spatial distribution of vulnerable buildings in three parts of Erbil city. By having the detailed information of the buildings, this approach can be used as an effective approach of early warning system to warn the residents of buildings that are at risk prior to the flood events with very high spatial accuracy. Moreover, the population in Erbil city has been estimated in order to determine the number of people at risk of flooding. For 2023 there were estimated of 882000 people in Erbil city, with population density of 917 people/km2. The result analysis showed that 33853 (3.84%) and 69258 (7.85%) of residents in Erbil city were located in very high and high risk flood zones, respectably. Around

quarter of populations with 27% (238426 residents) were in medium flood risk zones, and majority of residents 61% (539999 residents) were in low flood risk areas (Fig. 7).

One of the main reasons of flooding in Erbil city is the exceeding of the capacity of sewers during heavy rainstorms, leading to overloaded sewers due to massive water flow. However, insufficient design of drainage channel, inadequate maintenance of sewerage infrastructure, and blockages caused by debris carried by floodwaters are further contributors to flooding (K Sissakian, Al-Ansari et al. 2022). Flood mitigation strategies and regular cleaning of the sewerage lines significantly reduce the hazards related to flood and save infrastructures and peoples life in flood prone areas. Despite the fact that the government entities and policy makers planned to implement various techniques to reduce the flood hazards in 2022 by constructing 40 dams, ponds, and canals with more than 28 million dollars budget, however, due to the unpredictability of weather patterns, the fully flood prevention in Erbil city and other parts of the Kurdistan region is still a challenging issue. Moreover, sewer system cleaning and maintenance before rainy seasons regularly implemented by the government entities as one of the significant flood prevention measures. Furthermore, public awareness campaigns and informing residents for proper waste disposal approaches critically contribute to the reduction of blockages of sewerage systems (www.wishe.net).

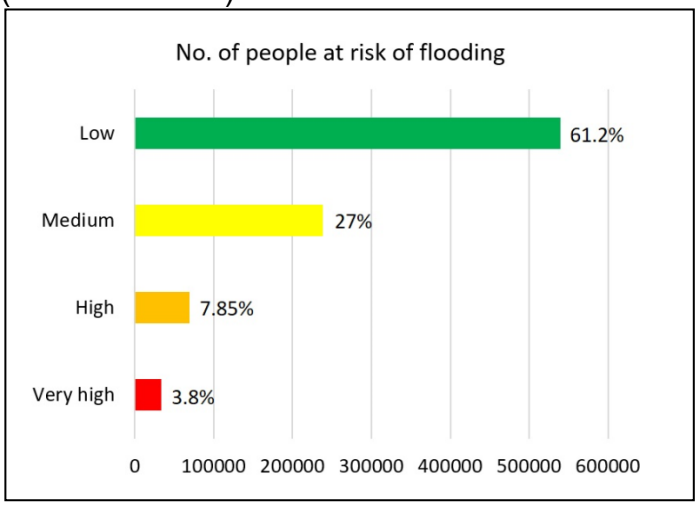

Figure 6: Estimated number of people at risk of flooding based on FSM.

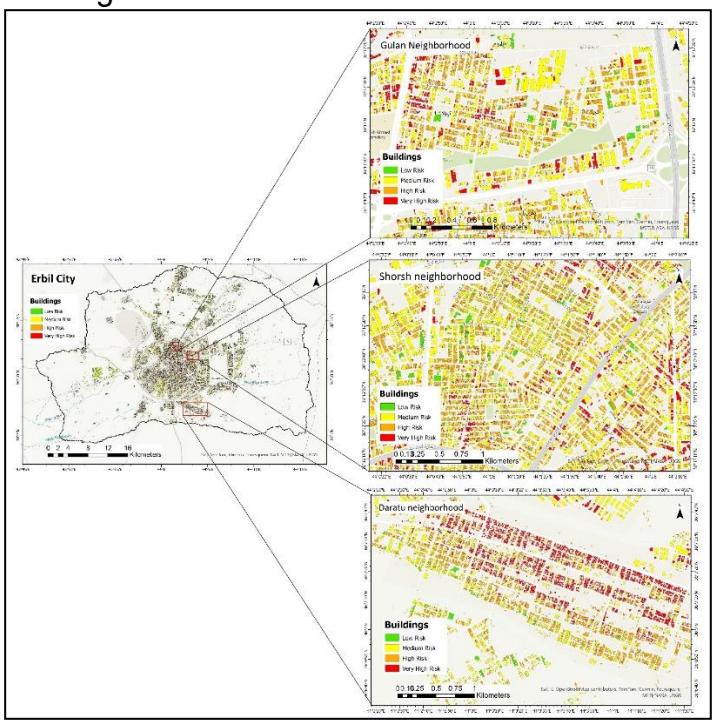

Figure 7: Vulnerable buildings of three parts in Erbil city: Gulan (a), Shorsh (b) and Daratu (c) neighborhoods.

3.4. Recommendations

For enhancing flood prediction modelling, it's suggested that future studies benefit in using the integration of machine learning and deep learning techniques with GIS in Erbil and similar environments. Also, using real-time rainfall data and the identified flood-prone areas could aid notably in determining urban building flood vulnerability to develop an early warning system to alert residents prior the flood events. Additionally, future researches could focus on implementing comprehensive and efficient investigation of different flood mitigation strategies, particularly in regions identified as high and very high flood risk areas in Erbil city. Furthermore, it's essential to examine the effectiveness of the newly constructed dams and ponds and their impact on flood risk mitigations, and identifying the essential infrastructure improvements to investigate the detailed analyse the flood hazards contribution to the urban drainage system capacity.

Conclusions

GIS and remote sensing technologies with integrations of AHP technique significantly

contributed in better understanding the flood hazards, specifically in urban regions. GIS and remote sensing techniques with AHP methodology were utilized in this research to assess the flood susceptible areas using 14 different factors. The results showed that 109 km2 (12.1%) of Erbil city area located in high and very high flood risk areas. Additionally, results notably showed that nearly half of buildings in Erbil city with 47.6% are located in high and very high flood risk areas, underscoring the urgent need for mitigation planning and flood management measures. Moreover, the significant results illustrated that 103111 (11.69 %) of residents in Erbil city were located in very high and high risk flood zones combined. The accuracy of produced flood susceptibility map were assessed using 41 points of historical floods. The assessment showed that 92.5% of historical floods were located in very high flood susceptible areas, and the accuracy of AUC-ROC curve was 92.2%, emphasizing the reliability of AHP technique for assessing flood hazards. The proposed approach in this study significantly contribute in flood hazard analysis and aiding early warning system development to reduce the impacts of flood events. As the Erbil city expands more in multiple directions, which leads to more land use feature alteration and changing the natural drainage system conditions, future urban planning and policy making processes should consider the flood susceptible areas to foster more sustainable urbanization and reduce the severe impacts of flood hazards. The approach used in this study offers valuable tools and insights for policy makers and urban planners to better understand flood hazards and implement better mitigation strategies, additionally, the approach can be applied to similar urban regions which experience same challenges of Erbil city. Hence, this study recommend to implement versatile framework to monitor the flood events and analyze the factors contributed in flood events, specifically in Daratu, Khabat and Newroz neighborhoods. Additionally, fostering greener infrastructure in dense population areas and improving natural runoff could significantly reduce the impacts of flood hazards to have more sustainable environmental conditions in Erbil city. Policy makers could assess the flood risk areas periodically with enhancement methodologies which aids critically in long term flood management for similar urban conditions. The building vulnerability assessment and mapping can be used as a base for improving emergency response planning and developing early warning system, ensuring the long term safety of urban populations and infrastructures.

Acknowledgment: The authors gratefully acknowledge Salahaddin University - Erbil for its invaluable institutional and academic support throughout the course of this research.

Financial support: This research was financially supported by Salahaddin University - Erbil.

Potential conflicts of interest. All authors report no conflicts of interest relevant to this article.

References

Abrar, M.F., Iman, Y.E., Mustak, M.B. and Pal, S.K., 2024. Assessment of vulnerability to flood risk in the Padma River Basin using hydro-morphometric modeling and flood susceptibility mapping. Environmental Monitoring and Assessment, 196(7), p.661.

Adedoja, T.B., Popoola, O.S., Alaga, T.A. and Akindejoye-Adesioye, A.E., 2023. Flood vulnerability mapping: a case study of Okoko Basin, Osogbo. Journal of Geographic Information System, 15(5), pp.580-596.

Akhtar, Z., Sajjad, M., Imran, M. and Ofli, F., 2023. Risk Mapping in Managing Flood Vulnerability in Disaster Management. In International Handbook of Disaster Research (pp. 743-776). Singapore: Springer Nature Singapore.

Al-Omari, A.A., Shatnawi, N.N., Shbeeb, N.I., Istrati, D., Lagaros, N.D. and Abdalla, K.M., 2024. Utilizing remote sensing and GIS techniques for flood hazard mapping and risk assessment. Civil Engineering Journal, 10(5), pp.1423-1436.

Al-Sababhah, N., 2023. Detection of flood-hazard-prone zones using GIS modeling and AHP method in urban areas: the case of Amman Governorate. Bulletin of Geography. Physical Geography Series, (24).

Al–Shwani, J.K.M., Saleh, S.A. and Al-Manmi, D.A.M.A., 2025. Identifying Areas Exposed to Potential Flash Floods and Drawing Map for Them Using Multi-Criteria Decision-Making Depending on GIS and AHP for Erbil Sub-Basin, Northern Iraq.

Ali, B.A. and Mawlood, D.K., 2023. Applying the SWMM Software Model for the High Potential Flood-Risk Zone for Limited Catchments in Erbil City Governorate. Zanco Journal of Pure and Applied Sciences, 35(4), pp.41-50.

Ali, B.A. and Mawlood, D.K., 2023. Urban Flood Simulation in Erbil City by Using Storm Water Management Model

(SWMM). Zanco Journal of Pure and Applied Sciences, 35(5), pp.1-11.
Allafta, H. and Opp, C., 2021. GIS-based multi-criteria analysis for flood prone areas mapping in the trans-boundary Shatt Al-Arab basin, Iraq-Iran. Geomatics, Natural Hazards and Risk, 12(1), pp.2087-2116.
Askar, S., Zeraat Peyma, S., Yousef, M.M., Prodanova, N.A., Muda, I., Elsahabi, M. and Hatamiafkoueieh, J., 2022. Flood susceptibility mapping using remote sensing and integration of decision table classifier and metaheuristic algorithms. Water, 14(19), p.3062.
Aziz, S.Q., Saleh, S.M., Muhammad, S.H., Ismael, S.O. and Ahmed, B.M., 2023. Flood Disaster in Erbil City: Problems and Solutions. Environmental Protection Research, pp.303-318.
Azizah, V., Deffinika, I. and Arinta, D., 2022, July. The effect of land use changes on land surface temperature in malang city's on 2016-2020. In IOP Conference Series: Earth and Environmental Science (Vol. 1066, No. 1, p. 012006). IOP Publishing.
Benítez, J., Delgado-Galván, X., Izquierdo, J. and Pérez-García, R., 2012. An approach to AHP decision in a dynamic context. Decision Support Systems, 53(3), pp.499-506.
Bouaziz, M., Eisold, S. and Guermazi, E., 2017. Semiautomatic approach for land cover classification: a remote sensing study for arid climate in southeastern Tunisia. Euro-Mediterranean Journal for Environmental Integration, 2(1), p.24.
Bui, Q.D., Luu, C., Mai, S.H., Ha, H.T., Ta, H.T. and Pham, B.T., 2023. Flood risk mapping and analysis using an integrated framework of machine learning models and analytic hierarchy process. Risk Analysis, 43(7), pp.1478-1495.
Buringh, P., 1957. Exploratory soil map of Iraq. Ministry of Agriculture, Baghdad.
Cabrera, J.S. and Lee, H.S., 2019. Flood-prone area assessment using GIS-based multi-criteria analysis: A case study in Davao Oriental, Philippines. Water, 11(11), p.2203.
Celone, M., Pecor, D.B., Potter, A., Richardson, A., Dunford, J. and Pollett, S., 2022. An ecological niche model to predict the geographic distribution of Haemagogus janthinomys, Dyar, 1921 a yellow fever and Mayaro virus vector, in South America. PLOS Neglected Tropical Diseases, 16(7), p.e0010564.
Chen, W. and Samuelson, F.W., 2014. The average receiver operating characteristic curve in multireader multicase imaging studies. The British journal of radiology, 87(1040), p.20140016.
Chomani, K., 2023. Assessing the impact of urbanization on flood hazards in Ranya city, using GIS and remote sensing. EURASIAN JOURNAL OF SCIENCE AND ENGINEERING, 9(3), pp.154-165.
Chomani, K., 2024. Evaluating the COVID-19 Lockdown's Effects on Land Surface Temperature, NO2, and O3 in the Erbil City, Kurdistan Region of Iraq. Cihan University-Erbil Scientific Journal, 8(2), pp.84-92.
Chomani, K. and Manguri, S.B.H., 2024. Spatiotemporal Insights into Ranya's Land-Use Transformation using Time-Series Imagery. Polytechnic Journal, 14(1), p.9.
Chomani, K. and Pshdari, S., 2024. Evaluation of Different Classification Algorithms for Land Use Land Cover Mapping. Kurdistan Journal of Applied Research, 9(2), pp.13-22.
D'Allestro, P. and Parente, C., 2015. GIS application for NDVI calculation using Landsat 8 OLI images. International Journal of Applied Engineering Research, 10(21), pp.42099-42102.
Dano, U.L., Balogun, A.L., Matori, A.N., Wan Yusouf, K., Abubakar, I.R., Said Mohamed, M.A., Aina, Y.A. and Pradhan, B., 2019. Flood susceptibility mapping using GIS-based analytic network process: A case study of Perlis, Malaysia. Water, 11(3), p.615.
Das, S. and Pardeshi, S.D., 2018. Morphometric analysis of Vaitarna and Ulhas river basins, Maharashtra, India: using geospatial techniques. Applied Water Science, 8(6), p.158.
Dawood, A.H. and Mawlood, D.K., 2023. Flood Risk Analysis in Potential Points, Zerin City in Erbil as a Case Study. The Iraqi Geological Journal, pp.182-193.
Dawood, A.H., Mawlood, D.K. and Al-Ansari, N., 2021. Flood Modeling on Koya Catchment Area Using Hyfran, Web Map Service, and HEC-RAS Software. ARO-The Scientific Journal of Koya University, 9(2), pp.107-111.
Desalegn, H. and Mulu, A., 2021. Flood vulnerability assessment using GIS at Fetam watershed, upper Abbay basin, Ethiopia. Heliyon, 7(1).
Diaconu, D.C., Costache, R. and Popa, M.C., 2021. An overview of flood risk analysis methods. Water, 13(4), p.474.
Diriba, D., Takele, T., Karuppannan, S. and Husein, M., 2024. Flood hazard analysis and risk assessment using remote sensing, GIS, and AHP techniques: a case study of the Gidabo Watershed, main Ethiopian Rift, Ethiopia. Geomatics, Natural Hazards and Risk, 15(1), p.2361813.
Dwivedi, L., Pandey, R. and Tripathi, S., 2022. Remote sensing and GIS based morphometric characterization of Bichiya river watershed of Rewa district, MP. International Journal of Applied Research, 8(6), p.101.
Eryani, I.G.A.P., Jayantari, M.W. and Ramli, S., 2024. Determination of flood vulnerability level based on different numbers of indicators using AHP-GIS. SINERGI, 28(1), pp.13-22.
Fatah, K.K. and Mustafa, Y.T., 2022. Flood susceptibility mapping using an analytic hierarchy process model based on remote sensing and GIS approaches in Akre District, Kurdistan Region, Iraq. The Iraqi Geological Journal, pp.123-151.
Ghosh, D.K., Mandal, A.C., Majumder, R., Patra, P. and Bhunia, G.S., 2018. Analysis for mapping of built-up area using remotely sensed indices–A case study of Rajarhat Block in Barasat Sadar Sub-Division in West Bengal (India). Journal of Landscape Ecology, 11(2), pp.67-76.

Hariyono, M.I. and Kurniawan, A.A., 2022, September. The use of digital elevation model in a GIS for flood vulnerability: Case study of Sitiarjo Village Malang District East Java Indonesia. In IOP conference series: Earth and environmental science (Vol. 1039, No. 1, p. 012020). IOP Publishing.

Hoque, M.A.A., Tasfia, S., Ahmed, N. and Pradhan, B., 2019. Assessing spatial flood vulnerability at Kalapara Upazila in Bangladesh using an analytic hierarchy process. Sensors, 19(6), p.1302.

Huu Duy, N., Tuan Pham, L., Xuan Linh, N., Van Truong, T., Dang, D.K., Quang Hai, T. and Bui, Q.T., 2024. Flood risk assessment using machine learning, hydrodynamic modelling, and the analytic hierarchy process. Journal of Hydroinformatics, 26(8), pp.1852-1882.

Ibeabuchi, U., 2023. Lagos' Vulnerability to Flood's Changes Mapping Adopting Analytical Hierarchy Process Using Geographical Information System. Indonesian Journal of Multidisciplinary Science, 2(6), pp.2589-2608.

Ibrahim, J.R., 2021. Estimating the hazards of floods in the Gulasur Basin in the Sulaymaniyah Governorate-Kurdistan Region of Iraq. Journal of University of Anbar for Humanities, 2(2).

Ibrahim Mahmoud, M., Duker, A., Conrad, C., Thiel, M. and Shaba Ahmad, H., 2016. Analysis of settlement expansion and urban growth modelling using geoinformation for assessing potential impacts of urbanization on climate in Abuja City, Nigeria. Remote Sensing, 8(3), p.220.

Iliadis, C., Galiatsatou, P., Glenis, V., Prinos, P. and Kilsby, C., 2023. Urban flood modelling under extreme rainfall conditions for building-level flood exposure analysis. Hydrology, 10(8), p.172.

Jiménez-Valverde, A., 2012. Insights into the area under the receiver operating characteristic curve (AUC) as a discrimination measure in species distribution modelling. Global Ecology and Biogeography, 21(4), pp.498-507.

Johnston, K., Ver Hoef, J.M., Krivoruchko, K. and Lucas, N., 2001. Using ArcGIS geostatistical analyst (Vol. 380). Redlands: Esri.

Sissakian, V.K., Al-Ansari, N., Adamo, N., Abdul Ahad, I.D. and Abed, S.A., 2022. Flood hazards in erbil City Kurdistan region Iraq, 2021: A case study. Engineering, 14(12), pp.591-601.

Kara, R. and Singh, P., 2024. Flood assessment for Lower Godavari basin by using the application of GIS-based analytical hierarchy process. International Journal of System Assurance Engineering and Management, pp.1-23.

Kaya, C.M. and Derin, L., 2023. Parameters and methods used in flood susceptibility mapping: a review. Journal of Water and Climate Change, 14(6), pp.1935-1960.

Khaddari, A., Jari, A., Chakiri, S., El Hadi, H., Labriki, A., Hajaj, S., El Harti, A., Goumghar, L. and Abioui, M., 2023. A comparative analysis of analytical hierarchy process and fuzzy logic modeling in flood susceptibility mapping in the Assaka Watershed, Morocco. Journal of Ecological Engineering, 24(8), pp.62-83.

Khaldi, L., Elabed, A. and El Khanchoufi, A., 2023. Quantitative assessment of the relative impacts of different factors on flood susceptibility modelling: case study of Fez-Meknes region in Morocco. In E3S Web of Conferences (Vol. 364, p. 02005). EDP Sciences.

Khoeun, C., Sok, T., Chan, R., Khe, S., Ich, I., Chan, K. and Oeurng, C., 2022, November. Assessing Flood Hazard Index using Analytical Hierarchy Process (AHP) and Geographical Information System (GIS) in Stung Sen River Basin. In IOP Conference Series: Earth and Environmental Science (Vol. 1091, No. 1, p. 012031). IOP Publishing.

Klingenstein, A., Haritoglou, I., Schaumberger, M.M., Nentwich, M.M., Hein, R. and Schaller, U.C., 2011. Receiver operating characteristic analysis: calculation for the marker 'melanoma inhibitory activity'in metastatic uveal melanoma patients. Melanoma research, 21(4), pp.352-356.

Kohen, J., 1960. A coefficient of agreement for nominal scale. Educ Psychol Meas, 20, pp.37-46.

Li, J., Zheng, A., Guo, W., Bandyopadhyay, N., Zhang, Y. and Wang, Q., 2023. Urban flood risk assessment based on DBSCAN and K-means clustering algorithm. Geomatics, Natural Hazards and Risk, 14(1), p.2250527.

Lin, P., Pan, M., Wood, E.F., Yamazaki, D. and Allen, G.H., 2021. A new vector-based global river network dataset accounting for variable drainage density. Scientific data, 8(1), p.28.

M Amen, A.R., Mustafa, A., Kareem, D.A., Hameed, H.M., Mirza, A.A., Szydłowski, M. and M. Saleem, B.K., 2023. Mapping of flood-prone areas utilizing GIS techniques and remote sensing: a case study of Duhok, Kurdistan Region of Iraq. Remote Sensing, 15(4), p.1102.

Magureanu, M., Sfîrcoci, M., Copacean, L. And Cojocariu, L., 2023. Flood Risk Of Grasslands In The Mountain Area Of Western Romania. Life Science And Sustainable Development, 4(1), Pp.111-119.

Manfreda, S., Samela, C. and Troy, T.J., 2017. The use of DEM-based approaches to derive a priori information on flood-prone areas. In Flood monitoring through remote sensing (pp. 61-79). Cham: Springer International Publishing.

Mechentel, E., Dairi, S., Djebbar, Y. and HAMMAR, Y., 2024. Flash flood risk mapping using Analytic Hierarchy Process and machine learning: case of Souk-Ahras City, Northeastern Algeria.

Megahed, H.A., Abdo, A.M., AbdelRahman, M.A., Scopa, A. and Hegazy, M.N., 2023. Frequency ratio model as tools for flood susceptibility mapping in urbanized areas: A case study from Egypt. Applied Sciences, 13(16), p.9445.

Membele, G.M., Naidu, M. and Mutanga, O., 2022. Examining flood vulnerability mapping approaches in developing countries: A scoping review. International Journal of Disaster Risk Reduction, 69, p.102766.

Mikail, A.Q. and Hamad, R., 2023. Mapping Flood Vulnerability by Applying EBF And AHP Methods, in the Iraqi Mountain Region. Science Journal of University of Zakho, 11(1), pp.1-10.

Mishra, R., Pundir, A.K. and Ganapathy, L., 2017. Evaluation and prioritisation of manufacturing flexibility alternatives using integrated AHP and TOPSIS method: Evidence from a fashion apparel firm. Benchmarking: An International Journal, 24(5), pp.1437-1465.

Moharir, K., Singh, M., Pande, C.B. and Varade, A.M., 2024. GIS Based Delineation of Flood Susceptibility Mapping Using Analytic Hierarchy Process in East Vidarbha Region, India. In Geospatial Practices in Natural Resources Management (pp. 305-329). Cham: Springer International Publishing.

Mokhtari, E., Abdelkebir, B., Djenaoui, A. and Hamdani, N.E.H., 2024. Integrated analytic hierarchy process and fuzzy analytic hierarchy process for Sahel watershed flood susceptibility assessment, Algeria. Water Practice & Technology, 19(2), pp.453-475.

Mujib, M.A., Apriyanto, B., Kurnianto, F.A., Ikhsan, F.A., Nurdin, E.A., Pangastuti, E.I. and Astutik, S., 2021. Assessment of flood hazard mapping based on analytical hierarchy process (AHP) and GIS: application in kencong district, jember regency, Indonesia.

Mukhtar, M.A., Shangguan, D., Ding, Y., Anjum, M.N., Banerjee, A., Butt, A.Q., Li, D., Yang, Q., Khan, A.A., Muhammad, A. and He, B.B., 2024. Integrated flood risk assessment in Hunza-Nagar, Pakistan: unifying big climate data analytics and multi-criteria decision-making with GIS. Frontiers in Environmental Science, 12, p.1337081.

Mushtaq, F., Mahmood, K., Hamid, M.C. and Tufail, R., 2021. A Comparative Study of Support Vector Machine and Maximum Likelihood Classification to Extract Land Cover of Lahore District, Punjab, Pakistan. Pakistan Journal of Scientific & Industrial Research Series A: Physical Sciences, 64(3), pp.265-274.

Mustafa, A., Szydłowski, M., Veysipanah, M. and Hameed, H.M., 2023. GIS-based hydrodynamic modeling for urban flood mitigation in fast-growing regions: a case study of Erbil, Kurdistan Region of Iraq. Scientific reports, 13(1), p.8935.

Mustafa, B.Y., Faisal, M.D., Roeland, D.W., Ahmed, A.R. and Arbili, M.M., 2025. Flash Flood Hazard Mapping Using Analytical Hierarchy Process (AHP) and GIS Application: In the Barzan Area of Iraqi Kurdistan Region. Zanco Journal of Pure and Applied Sciences, 37(1), pp.108-125.

Nguyen, H.N., Fukuda, H. and Nguyen, M.N., 2024. Assessment of the Susceptibility of Urban Flooding Using GIS with an Analytical Hierarchy Process in Hanoi, Vietnam. Sustainability, 16(10), p.3934.

Osman, S.A. and Das, J., 2023. GIS-based flood risk assessment using multi-criteria decision analysis of Shebelle River Basin in southern Somalia. SN Applied Sciences, 5(5), p.134.

Ozkan, S.P. and Tarhan, C., 2016. Detection of flood hazard in urban areas using GIS: Izmir case. Procedia Technology, 22, pp.373-381.

Panday, D., Maharjan, B., Chalise, D., Shrestha, R.K. and Twanabasu, B., 2018. Digital soil mapping in the Bara district of Nepal using kriging tool in ArcGIS. PloS one, 13(10), p.e0206350.

Qi, W., Ma, C., Xu, H., Chen, Z., Zhao, K. and Han, H., 2021. A review on applications of urban flood models in flood mitigation strategies. Natural Hazards, 108, pp.31-62.

Ray, S.K., 2024. Flood risk index mapping in data scarce region by considering GIS and MCDA (FRI mapping in data scarce region by considering GIS and MCDA). Environment, Development and Sustainability, pp.1-53.

Saaty, T.L. and Vargas, L.G., 2012. Models, methods, concepts & applications of the analytic hierarchy process (Vol. 175). Springer Science & Business Media.

Samansiri, S., Fernando, T. and Ingirige, B., 2022. Advanced technologies for offering situational intelligence in flood warning and response systems: A literature review. Water, 14(13), p.2091.

Sarmah, T. and Das, S., 2018. Urban flood mitigation planning for Guwahati: A case of Bharalu basin. Journal of environmental management, 206, pp.1155-1165.

Shivhare, V., Kumar, A., Kumar, R., Shashtri, S., Mallick, J. and Singh, C.K., 2024. Flood susceptibility and flood frequency modeling for lower Kosi Basin, India using AHP and Sentinel-1 SAR data in geospatial environment. Natural Hazards, 120(13), pp.11579-11610.

Staponites, L. R., Barták, V., Bílý, M., and Simon, O. P., 2019. Performance of landscape composition metrics for predicting water quality in headwater catchments. Scientific reports 9(1), 14405.

Stevanovic, Z. M., M., 2003. Hydrogeology of Northern Iraq, Climate, Hydrology, Geomorphology & Geology. FAO 1, 1–122

Talha, S., Maanan, M., Atika, H., and Rhinane, H., 2019. Prediction of flash flood susceptibility using fuzzy analytical hierarchy process (Fahp) algorithms and Gis: a study case of guelmim region In Southwestern of Morocco. The international archives of the photogrammetry, remote sensing and spatial information sciences 42, 407-414.

Thannoun, R. G., and Ismaeel , O. A., 2024. Flood risk vulnerability detection based on the developing topographic wetness index tool in geographic information system. IOP Conference Series: Earth and Environmental Science, IOP Publishing.

Ullah, K., and Zhang, J., 2020. GIS-based flood hazard mapping using relative frequency ratio method: A case study of Panjkora River Basin, eastern Hindu Kush, Pakistan. Plos one 15(3), e0229153.

Vojtek, M., and Vojteková, J., 2019. Flood susceptibility mapping on a national scale in Slovakia using the analytical hierarchy process. Water 11(2), 364.

Yagoub, M., Alsereidi, A. A., Mohamed, E. A., Periyasamy, P., Alameri, R., Aldarmaki, S., and Alhashmi, Y., 2020. Newspapers as a validation proxy for GIS modeling in Fujairah, United Arab Emirates: identifying flood-prone areas. Natural Hazards 104, 111-141.

Zia, S., Shirazi, S. A., and Nasar-u-Minallah, M., 2021. Vulnerability assessment of urban floods in lahore, pakistan using gis based integrated analytical hierarchy approach: vulnerability assessment of urban floods in lahore. Proceedings of the Pakistan Academy of Sciences, A. Physical and Computational Sciences 58(1): 85-96.

Zzaman, R. U., Nowreen, S., Billah, M., and Islam, A. S., 2021. Flood hazard mapping of Sangu River basin in Bangladesh using multi-criteria analysis of hydro-geomorphological factors. Journal of Flood Risk Management 14(3), e12715.